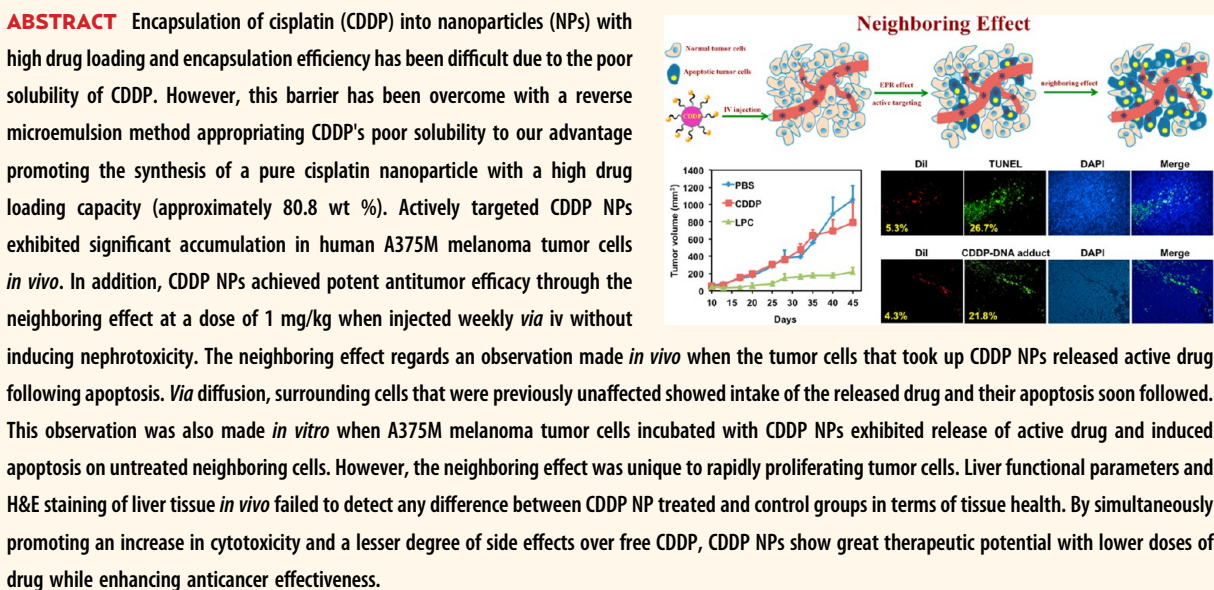


Lipid-Coated Cisplatin Nanoparticles Induce Neighboring Effect and Exhibit Enhanced Anticancer Efficacy

Shutao Guo, Yuhua Wang, Lei Miao, Zhenghong Xu, C. Michael Lin, Yuan Zhang, and Leaf Huang*

Division of Molecular Pharmaceutics and Center for Nanotechnology in Drug Delivery, Eshelman School of Pharmacy, University of North Carolina at Chapel Hill, Chapel Hill, North Carolina 27599, United States



KEYWORDS: cisplatin · chemotherapy · nanomedicine · drug delivery · neighboring effect

The use of cisplatin (CDDP) as a cytotoxic drug was pioneered by Rosenberg while studying the effects of electrical fields on the growth of bacteria.¹ Investigating the properties of platinum compounds, Rosenberg discovered that DNA damage induced by the cross-linking of CDDP and DNA initiates DNA repair mechanisms and triggers cell apoptosis when repair proves unsuccessful. Utilizing this interaction, CDDP has become a first-line therapy against a wide spectrum of solid neoplasms, including bladder, ovarian, colorectal and melanoma cancers.^{2,3} However, drug resistance and related systemic toxicities (e.g., nephro- and neurotoxicities) limit the clinical use of CDDP.^{4,5}

Formulating small molecule drugs into nanoparticles (NPs), such as liposomal or polymeric formulations, allows for a significant reduction of adverse side effects while

maintaining antitumor efficacy. Therefore, this class of nanomedicine is currently established as the cutting edge method in treating a variety of cancers.^{6,7} With modification, NPs are able to avoid undesired uptake by the reticuloendothelial system (RES) and improve circulation of their encapsulated drugs in the blood compared to free drug.⁸ Thus, drug efficacy can be greatly increased without a subsequent increase in collateral damage to healthy tissues.

Similarly, uptake of NPs by tumor cells can be mediated by tumor targeting ligands, such as aptamer,⁹ RGD peptide and anisamide (AA).^{10–12} The accumulation of nano-sized formulations in tumors is also highly dependent on the enhanced permeability and retention (EPR) effect due to the disorganized and tortuous tumor endothelium.¹³ Nonetheless, the accessibility of NPs into

* Address correspondence to leaf@unc.edu.

Received for review July 15, 2013 and accepted October 1, 2013.

Published online October 01, 2013
10.1021/nn403606m

© 2013 American Chemical Society

tumor cells primarily depends on the properties of the NPs, especially size. NPs with a diameter less than 50 nm can penetrate deeper into poorly permeable, hypo-vascular tumors with greater efficiency than larger NPs.^{14,15}

However, the poor solubility of inorganic CDDP in both water and oil significantly limits the development of NPs with high drug loading and encapsulation efficacy. In our previous study, lipid-coated CDDP (LPC) NPs composed entirely of CDDP and outer leaflet lipids were successfully synthesized and characterized with high drug loading capacity. Compared to other lipid-based cisplatin nanocapsules,^{16–18} LPC NPs were much smaller and more homogeneous in size.

Herein, we evaluated the anticancer efficacy of LPC NPs on A375M melanoma xenograft tumors. Furthermore, the *in vitro* release profile of LPC NPs in cells incubated in a medium with 50% fetal bovine serum was evaluated. Also, the diffusion and distance dependent neighboring effect of LPC NPs was additionally examined both *in vitro* and *in vivo*. Finally, the biodistribution and safety profile of LPC NPs was determined.

RESULTS AND DISCUSSION

Physiochemical Characterizations of LPC NPs. While the major side effects of CDDP can be minimized through the usage of NPs for drug delivery, the poor solubility of CDDP has hampered the development of a successful nanoparticulate formulation. In the present study, we have successfully synthesized lipid-coated, platinum-filled

drug formulations (LPC NPs) characterized with a core of CDDP and 80 wt % of drug loading. LPC NPs were negatively stained with uranyl acetate for transmission electron microscopy (TEM). The images revealed the core/membrane nanostructure of NPs with a size of approximately 20 nm in diameter (Figure 1A). DLS results (Figure 1B) further indicated that the hydrodynamic diameter of NPs was approximately 30 nm, slightly larger than the diameter observed in TEM images. The drug loading capacity of LPC NPs determined using inductively coupled plasma mass spectrometry (ICP-MS) was 80.8 wt %. Other liposomal formulations of CDDP based drugs, such as SPI-77 (6.7 wt %) and Lipoplatin (10 wt %), which are in phase II clinical trials and clinically approved, respectively, cannot achieve such high drug loading.¹⁹

LPC NPs Delivered CDDP Efficiently into A375M Cells and Show

Significant Efficacy. To test the anticancer efficacy of LPC NPs, we first evaluated the cytotoxicity of LPC NPs in A375M melanoma cancer cells. As shown in Figure 2A, the LPC NPs showed a nearly 10-fold lower IC_{50} than free drug (1.2 vs 10.2 μ M) regarding the growth inhibition in A375M cells. As a control, empty liposome vesicles did not induce any cytotoxicity (data not shown). Figure 2B,C quantitatively presented cellular uptake of NPs measured using ICP-MS. As indicated, LPC NPs delivered CDDP efficiently into A375M cells with a 6.5-fold increase in internalized drug over free CDDP. *In vitro* studies illustrated that LPC NPs efficiently transported CDDP into cells and resulted in a significantly lower IC_{50} over free CDDP.

LPC NPs Showed High Accumulation of CDDP in A375M

Xenograft Bearing Mice and Significant Antitumor Efficacy at a Low Dose. The biodistribution of free CDDP and LPC NPs in tumor-bearing mice was compared. Twenty-four hours post-iv injection, 10.5% of the injected dose per gram of LPC NPs accumulated in the tumors, which was significantly higher than the 1.2% of the injected dose per gram of free CDDP (Figure 3A). To determine the efficacy of LPC NPs in treating A375M tumors, the drugs were administered weekly by IV injection at a dose of 1.0 mg/kg Pt. LPC NPs inhibited the growth of A375M tumors significantly without reducing the body

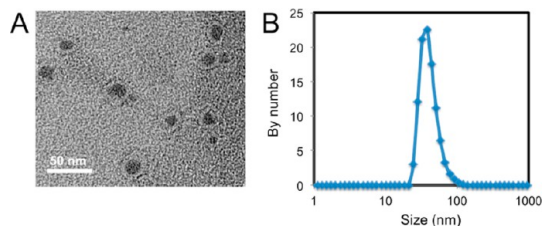


Figure 1. LPC NPs were characterized with a small size and narrow dispersity. (A) Characterization of LPC NPs using TEM. LPC NPs were negatively stained with uranyl acetate. Scale bar represents 50 nm. (B) Characterization of LPC NPs using dynamic light scattering (DLS).

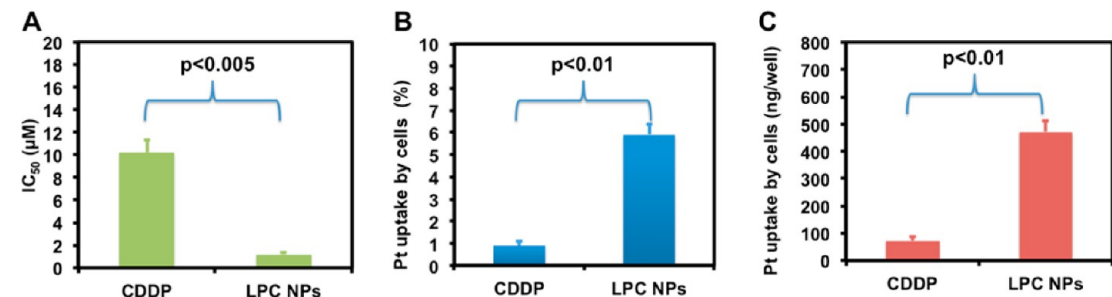


Figure 2. LPC NPs exhibited high toxicity and strong transport ability of CDDP. (A) IC_{50} of CDDP and LPC NPs in A375M cells. (B) The amount of cell uptake of CDDP and LPC NPs in A375M cells quantified using ICP-MS. Data is expressed as % uptake. (C) The amount of the Pt drug associated with cells after incubation with 100 μ M CDDP or LPC NPs in 24 well plates. Each bar represents the mean \pm SEM of 3 independent experiments. The analysis of variance is completed using a one-way ANOVA.

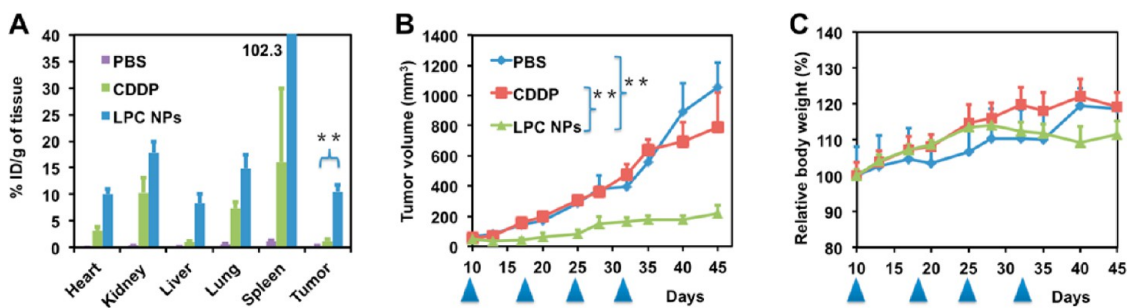


Figure 3. LPC NPs showed high accumulation in A375M tumor cells and impeded the growth of tumors at 1.0 mg/kg of Pt. (A) Pt distribution in A375M tumor bearing mice administered with CDDP and LPC NPs. One milligram per kilogram of Pt was administered weekly *via* iv injection. (B and C) Effects of CDDP and LPC NPs on tumor growth and body weight, respectively, of A375M tumor bearing mice. The arrowheads indicate the time of injection. The results are displayed as mean \pm SEM (error bars) of five animals per group. The analysis of variance is computed using a one-way ANOVA. Asterisks (**) indicates $p < 0.01$.

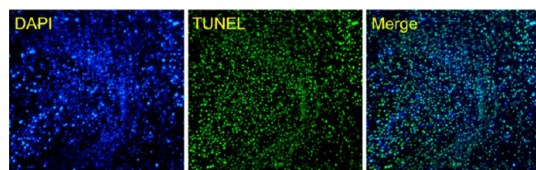


Figure 4. LPC NPs induced apoptosis in 90% of tumor cells. Effects of LPC NPs on A375M tumor cell apoptosis using TUNEL assay. The tumors were treated once a week for two weeks with iv injections containing 3.0 mg/kg of Pt.

weight of the treated animals (Figure 3B,C). However, free CDDP at the same dose and dosing schedule was ineffective, possibly due to a low tumor accumulation.

In vivo, the small size of LPC NPs facilitated the accumulation of LPC NPs in tumor cells through the EPR effect. Therefore, LPC NPs achieved an accumulation of 10.5% injected dose (ID)/g in A375M tumor cells and exhibited significant anticancer therapeutic effect at a low dose and generous dosing schedule, while free CDDP was ineffective at the same dose. LPC NPs are therefore capable of inducing considerable antitumor efficacy at a significantly lower dose than free CDDP and can be applied to treat a wide range of cancers.

LPC NPs Induced Discernible Apoptosis in A375M Tumors. After confirming that LPC NPs showed significant antitumor efficacy, an additional experiment was used to evaluate their efficacy in treating large tumors. Mice bearing A375M melanoma tumors of approximately 600 mm³ were dosed with iv administrations of LPC NPs at a dose of 3.0 mg/kg Pt once a week, for a period of two weeks. One week after the final injection, the mice were sacrificed and the tumors were assayed using TUNEL, a marker of apoptosis. As shown in Figure 4, about 90% of tumor cells were apoptotic, resulting in a 60% reduction in tumor volume (data not shown). Since it is highly unlikely that NPs can reach 90% of tumor cells, additional mechanisms must be contributing to the tumor reduction. The majority of apoptosis may actually be induced by the small fraction of cells that took up the NPs in a pattern known as the neighboring effect. This phenomenon is characterized as the uptake of NPs by tumor cells that become

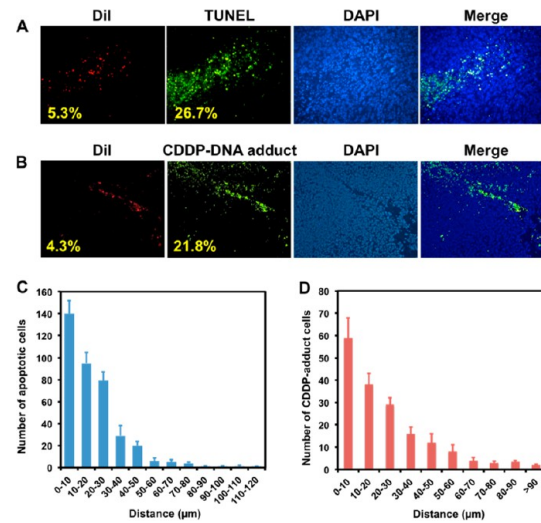


Figure 5. Neighboring effect was studied using TUNEL assay and detection of CDDP–DNA adduct. LPC NPs were labeled with Dil dye (red). The mice were sacrificed 24 h after receiving a single iv injection of LPC NPs at a dose of 1.0 mg/kg Pt. (A) The distribution of NPs was tracked by Dil dye, and the apoptotic tumor cells were detected by the TUNEL assay; (B) the formation of CDDP–DNA in tumor cells detected by CDDP–DNA antibody. (C) The number of TUNEL positive cells measured as a function of the distance to its nearest Dil positive cell; (D) the number of CDDP–DNA adduct positive cells measured as a function of the distance to its nearest Dil positive cell.

in situ drug depots and release active drugs to induce apoptosis in surrounding cells. Therefore, the neighboring effect is a distance and diffusion dependent effect.

Neighboring Effect Contributed to Significant *In Vivo* Apoptosis. In support of our hypothesis *in vivo*, we investigated the intracellular distribution of LPC NPs in tumors and tested the apoptosis of tumor cells using TUNEL and CDDP–DNA adduct antibody. To determine the mechanism of the neighboring effect, we used a lipophilic dye, 1,1'-dioctadecyl-3,3',3'-tetramethylindocarbocyanine perchlorate (Dil), to label LPC NPs. Dil was entrapped in an asymmetric bilayer. Results indicated that only 5.3% of the tumor cells took up the NPs and yet, 26.7% of cells underwent apoptosis (Figure 5A). It is possible that the amount of NPs in

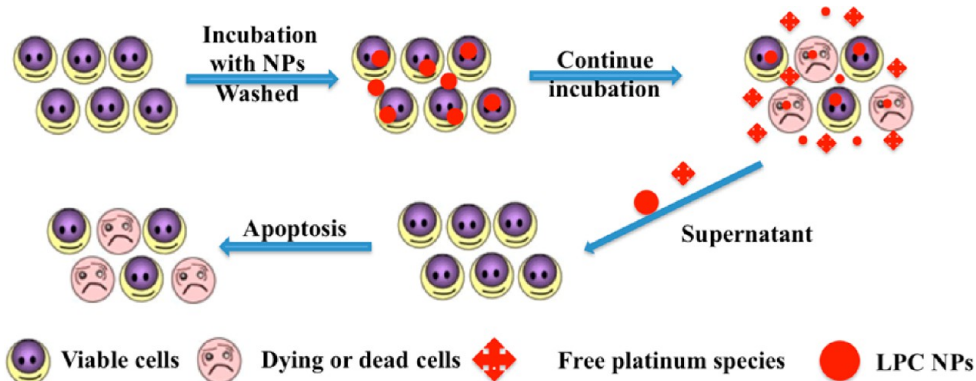


Figure 6. The procedures used to validate the neighboring effect *in vitro*.

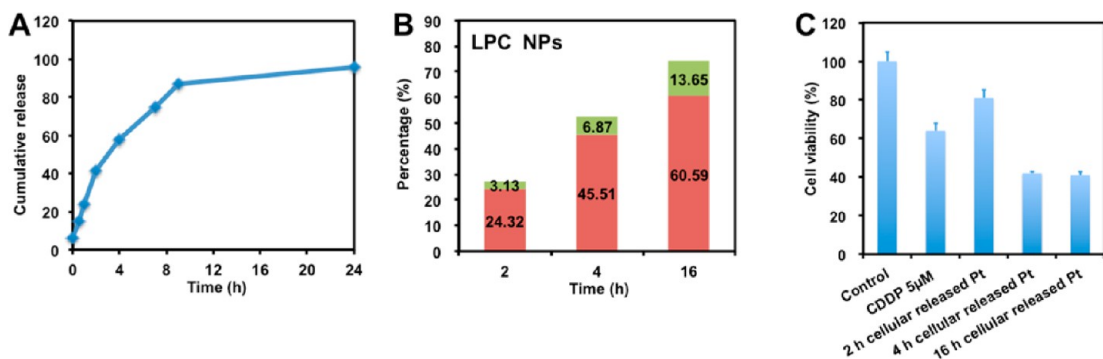


Figure 7. LPC NPs showed a controlled release pattern in medium and in cells. (A) *In vitro* release kinetics of encapsulated platinum in 50% FBS medium at 37 °C and the cellular release of Pt from LPC NPs treated cells. (B) Percentages of Pt in the released medium that were pelletable (green) and unpelletable (red) are shown. (C) The cytotoxic activity of released drugs from NP treated cells at different time points. Cells were treated with 5 μ M CDDP for comparison. Each bar represents the mean \pm SEM of 3 independent experiments.

some TUNEL positive cells was too low to be detected because of the detection limitations of the technique. Therefore, we used a “nearest neighbor” analysis to eliminate this possibility. The number of apoptotic cells was measured as a function of the distance to the nearest Dil positive cells. In groups treated with LPC NPs, the large number of green cells (TUNEL positive) close to red cells (Dil positive) gradually decayed to a small number of green cells far from red cells (Figure 5C). The data therefore indicated that the neighboring effect is indeed facilitated by diffusion and varies with distance from the depot cell.

In addition, an antibody specific to the Pt–DNA adduct was used in an assay for a nearest neighbor analysis to determine if Pt–DNA adduct was the cause of cell death.²⁰ As shown in Figure 5B, the formation of CDDP–DNA adducts was confirmed. It was consistently observed that a relatively small number of Dil-positive cells were able to induce the formation of the CDDP–DNA adduct in a large number of surrounding cells (Figure 5C,D). Therefore, formation of CDDP–DNA adduct is directly attributed to the release of CDDP *in vivo*. This data further provides strong evidence for the neighboring effect by suggesting that active Pt drugs released from dead or dying depot cells were diffused into previously unaffected cells.

In Vitro and Intracellular Release of Drugs from NPs and

Cytotoxicity Assays. To test the neighboring effect *in vitro* (Figure 6), intracellular release of CDDP from LPC NP was investigated. The kinetics regarding the release of platinum-based drugs from LPC NPs was evaluated in 50% FBS medium at 37 °C. As shown in Figure 7A, LPC NPs exhibited a sustained release of Pt over time with a half-life of 3.0 h.

We also labeled the NPs using fluorescent NBD-PE lipid and incubated them with cells. Some of the nanoparticles were co-localized with lysosomes as indicated by yellow spots (Figure S1). However, a large number of the NPs taken into the tumor cells did not co-localize with lysosomes.

We further tested the neighboring effect *in vitro* using the procedure shown in Figure 6. By culturing untreated cells with medium from LPC NPs treated cells, the activity of released CDDP was tested. Cells were first incubated with LPC NPs for 2, 4, or 16 h and subsequently washed and cultured. At different time points, the released, NPs and free drugs in the medium were separated by centrifugation at 16000g for 20 min. After centrifugation, we observed that the LPC NPs exhibited cellular release and that free drugs composed a major fraction of the medium (Figure 7B). To test the activity of drugs released from cells which

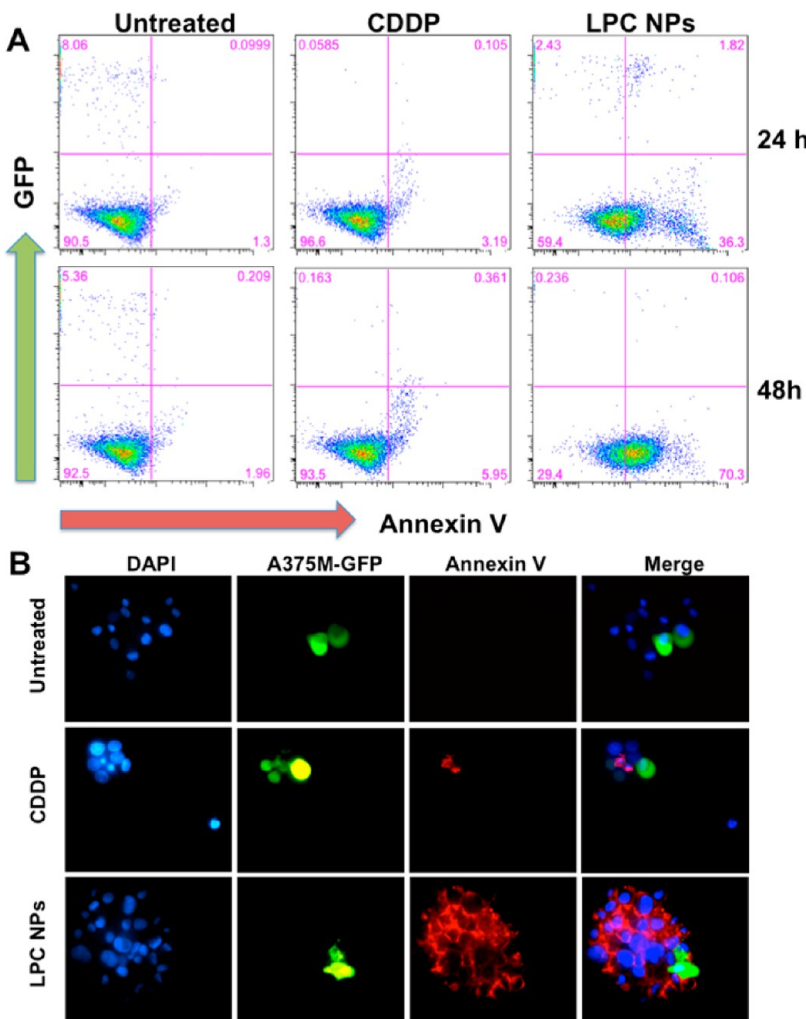


Figure 8. The neighboring effect demonstrated by coculturing CDDP transfected A375M-GFP cells and A375M cells at a 1:10 ratio. A375M-GFP cells were treated with LPC NPs (50 μ M) for 4 h. After 24 or 48 h of co-culturing, the cell nuclei were stained with Hoechst 33342 (blue). (A and B) Apoptotic cells were stained with Alexa Fluor 568-labeled Annexin V (red) for fluorescence microscopy and flow cytometry analysis.

previously entrapped NPs, the medium collected at different time points was transferred and incubated with untreated cells. After 48 h, the viability of the tumor cells was assayed using MTS. As shown in Figure 7C, the medium containing more drugs was more toxic.

Study of the Neighboring Effect *in Vitro*. In addition, we further investigated the neighboring effect using a common protocol. A375M-GFP cells that stably expressed green-fluorescence protein (green) were treated with 50 μ M of LPC NPs for 4 h, washed, and mixed with untreated A375M cells at a 1:10 ratio. Cells were incubated for an additional 24 or 48 h. Then, cell apoptosis was examined with Alexa Fluor 568-labeled Annexin V (red), an apoptosis marker.

In Figure 8A,B, many cells that were near the green, NP-treated cells were undergoing apoptosis. Groups treated with LPC NPs exhibited a pronounced effect while cells treated with CDDP showed only minimal signs of the neighboring effect. The apoptosis results were further quantified using flow cytometry. Cells

were analyzed at 24 (upper panels) or 48 (lower panels) h (Figure 8A). Untreated cells served as the control; after 24 or 48 h, A375M-GFP cells survived, while cells treated with CDDP died and disappeared at both time points. Furthermore, at 24 or 48 h the CDDP-treated cells did not induce significant apoptosis in the unlabeled and untreated cells. At 48 h, less than 6% of untreated cells were apoptotic. In contrast, cells treated with LPC NPs induced a higher percent of apoptotic cells, which were not directly exposed to CDDP. At 48 h, few green cells were left in both cases, but 70% apoptotic cells appeared in the untreated cell population for LPC NPs. It demonstrated that CDDP released from dead or dying cells was able to induce apoptosis on untreated tumor cells. These results confirm that the neighboring effect as characterized by the release of active drug from dead or dying cells after NP internalization and subsequent apoptosis in previously unaffected cells was validated both *in vivo* and *in vitro*. The cells transfected with NPs do, in fact, serve as drug

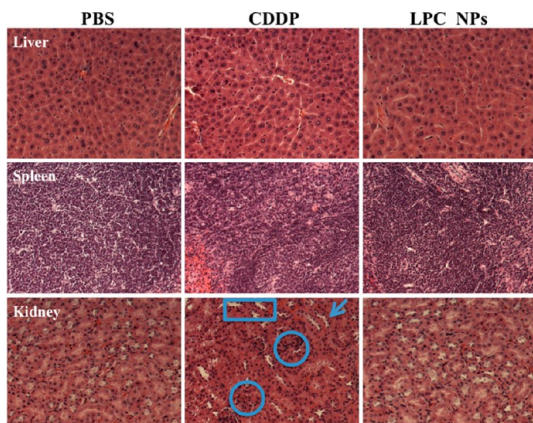


Figure 9. HE staining showed LPC NPs did not induce nephrotoxicity. H&E staining of liver, spleen, and kidney tissue from mice that received four doses of treatment (1 mg/kg each).

depots and affect the untreated cells in a manner dependent on distance and diffusion. Though the detailed mechanism behind the transport of the drugs from the depot cells to other cells is still unknown, we will continue to investigate the mechanism of the neighboring effect.

Safety Evaluations: LPC NPs Are Safe and No Neighboring Effect Is Observed in Major Organs. Although the neighboring effect displayed profound effects against rapidly proliferating tumor cells, its potential toxicity toward normal organs is of concern. Therefore, mechanism of the neighboring effect in normal tissues was studied. Since the liver was characterized as the major organ affecting clearance of NPs, the functional parameters aspartate transaminase (AST) and aspartate aminotransferase (ALT) of liver cells treated with free CDDP or LPC NPs were studied. The data indicated that the AST and ALT functional parameters from mice treated with CDDP and LPC NPs fell within the normal range (Figure S2). Furthermore, the comparison between H&E stained liver cells treated with LPC NPs and PBS displayed negligible differences in morphology (Figure 9). Therefore, LPC NPs only posed a minimal threat to normal liver function, which was probably due to the strong repair ability of cisplatin-induced DNA damage in the liver.^{21–23}

In addition, it was shown that Kupffer cells were responsible for harmlessly removing most of the NPs in the liver (Figure 10), while hepatocytes showed minimal LPC NPs uptake. Therefore, while the formation of the CDDP–DNA adduct was observed in some liver cells (Figure 11), subsequent apoptosis was not noted (Figure 12). This observation could be due to the successful repair of CDDP–DNA adducts which has been reported in previous works.^{21–23} This pattern was also found in other critical organs such as the kidney, spleen, heart, and lung.

Because the spleen was responsible for significant NP uptake (Figure 3A), histological analysis of the spleen was also performed to exclude any spleen toxicity induced by the NPs (Figure 9). Although LPC

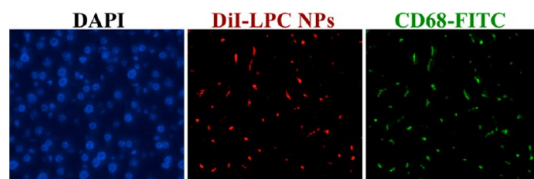


Figure 10. Dil-labeled LPC NPs (red) in liver were mainly taken up by Kupffer cells. Kupffer cells were stained using CD68 antibody (green) and the hepatocyte nuclei were stained using DAPI (blue). The mice were sacrificed 24 h after receiving a single iv injection of LPC NPs at a dose of 1.0 mg/kg Pt.

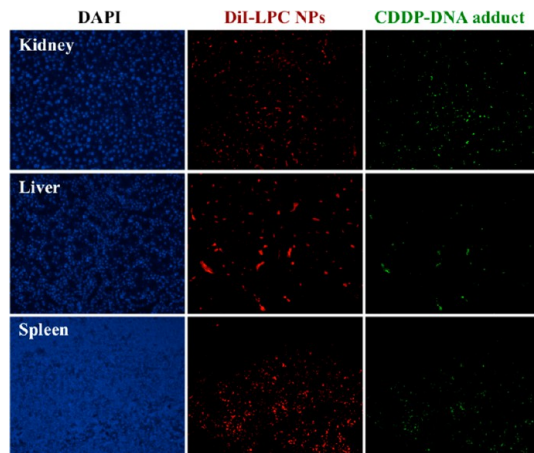


Figure 11. Although CDDP–DNA adducts were detected in kidney, liver and spleen, no neighboring effect is observed. The distribution of Dil-labeled LPC NPs (red) and the detection of CDDP–DNA adduct (green) in kidney, liver, and spleen. The mice were sacrificed 24 h after receiving a single iv injection of LPC NPs at a dose of 1.0 mg/kg Pt.

NPs accumulated 6-fold higher in the spleen than in cisplatin-treated mice as shown in Figure 3A, the data in Figure 12 indicated that LPC NPs did not induce significant apoptosis in spleen cells, which was consistent with other formulations.^{24,25} It is believed that uptake was performed primarily by macrophages which can successfully internalize the NP to prevent cell apoptosis (Figure 12). Therefore, the repair of CDDP–DNA adduct was also observed in spleen.

In clinics, the use of CDDP is mainly limited by nephrotoxicity. To this end, the nephrotoxicity of free CDDP and LPC NPs was studied. It was observed that LPC NPs induced significantly less nephrotoxicity over free CDDP at the same dose. As shown in Figure 9, the morphology of kidneys treated with LPC NPs was similar to that treated with PBS. Therefore, no signs of nephrotoxicity were observed in kidneys from mice treated with LPC NPs while some nephrotoxicity was observed in mice treated with free CDDP. Glomerulosclerosis, tubular cell atrophy, and cystic dilatation of renal tubes were observed in cells treated with free CDDP and indicated by rings, arrows, and squares, respectively. CDDP also induced significantly more apoptotic cells in kidney than in LPC NPs (Figure 12). In addition, there were no toxicities in heart and lung for both CDDP and LPC NPs. Pathologic examination of other

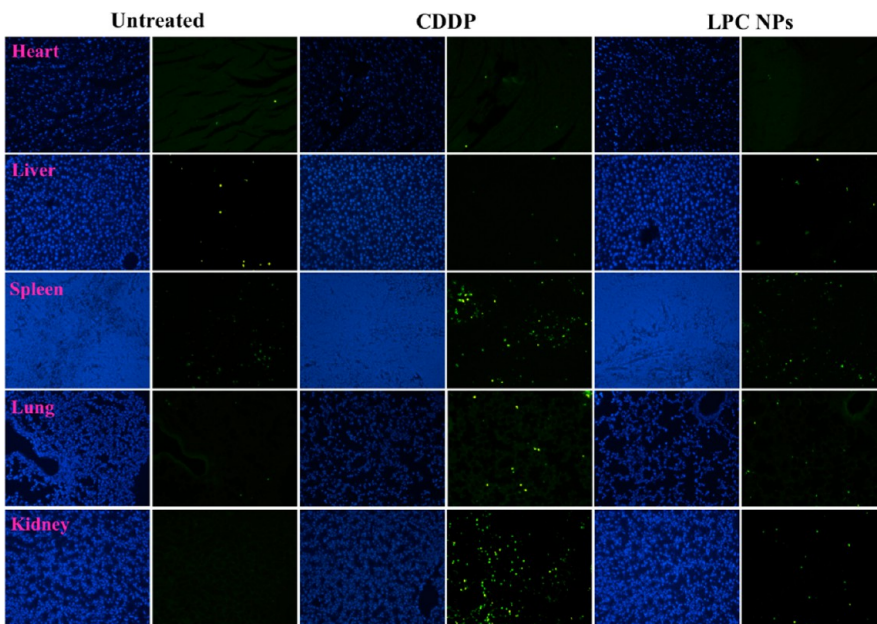


Figure 12. No significant apoptosis was detected in organs from LPC NPs treated mice. The detection of apoptotic cells in heart, liver, spleen, lung, and kidney using TUNEL assay is shown. The mice were sacrificed 24 h after receiving a single iv injection of LPC NPs at a dose of 1.0 mg/kg Pt. Apoptotic cells were detected using TUNEL assay (green) and the cell nuclei were stained using DAPI (blue).

major organs (lung and heart) in mice that received long-term treatments (Figure S3) indicated that mice treated with LPC NPs suffered no organ damage.

These results indicated that while the neighboring effect was capable of inducing high levels of apoptosis in cancerous cells, its effects on healthy cells were nearly unobservable. A similar pattern was also observed in heart and lung cells in mice treated with LPC NPs. A key mechanism behind this observation is the formation of Pt–DNA adducts in both cancerous and healthy cells alike. However, the Pt–DNA adducts could be successfully repaired in healthy cells while they induced observable apoptosis in cancerous cells. The specificity of these NPs therefore allows a significant antitumor effect to be achieved at a low dose and generous dosing schedule.

CONCLUSIONS

The antitumor efficacy of LPC NPs was tested *in vitro* and *in vivo*. When administered into mice at a low

weekly dose, LPC NPs effectively inhibited the growth of melanoma tumors while free CDDP proved ineffective at the same dose and dosing schedule. In addition, LPC NPs also exhibited the neighboring effect both *in vivo* and *in vitro*. The successful uptake of LPC NPs by the tumor cells and the release of active drug following apoptosis therefore furthers the effectiveness of the encapsulated drug. However, the neighboring effect was not induced in organ tissues due to their strong repair ability of the CDDP–DNA adduct. Thus, the tumor specific effect allows a magnification of anti-tumor efficacy at a low dose without pronounced side effects. Subsequently, both the therapeutic potential of CDDP and its safety toward normal tissues *in vivo* can be greatly optimized. Our studies have therefore distinguished the Pt drug delivery platform as an efficient and relatively safe candidate in the treatment of human melanoma tumors and a promising method for further explorations.

MATERIALS AND METHODS

Materials. All lipids were purchased from Avanti Polar Lipids (Alabaster, AL). DSPE-PEG-AA was synthesized in our laboratory as previously reported.¹⁰ CDDP, AgNO₃ and other chemicals were obtained from Sigma-Aldrich (St. Louis, MO) without further purification.

Cell Lines. The human melanoma, A375M, cell line was obtained from the American Type Culture Collection (ATCC, Manassas, VA). A375M-GFP was constructed by transfecting an A375M cell line with pEGFP-N1 plasmid. The episomal expression of the plasmid in the transfected cells was maintained by cultivating the cells in the media containing Neomycin. All cells were cultured in DMEM medium supplemented with 10%

heat-inactivated, fetal bovine serum (FBS), 20 mM of L-glutamine, 100 U/mL of penicillin G sodium, and 100 mg/mL of streptomycin at 37 °C in an atmosphere of 5% CO₂ and 95% air.

Preparations of LPC NPs. LPC NPs were synthesized according to our previous work.²⁶ Briefly, 200 mM *cis*-[Pt(NH₃)₂(H₂O)₂](NO₃)₂ and 800 mM KCl in water were separately dispersed in a solution composed of Cyclohexane/Igepal CO-520 (71:29, v/v) and Cyclohexane/Triton-X100/Hexanol (75:15:10, v/v/v) (3:1) to form a well-dispersed, water-in-oil reverse microemulsion. One hundred microliters of DOPA (20 mM) was added to the CDDP precursor phase and the mixture was stirred. Then, the two emulsions were mixed for another 30 min while the reaction proceeded. After that, ethanol was added to the microemulsion and the particles were collected by centrifugation at 12000g.

After being extensively washed with ethanol 2–3 times, the pellets were redispersed in 3.0 mL of chloroform and stored in a glass vial for further modification. Finally, 1.0 mL of LPC NPs core, 50 μ L of 20 mM DOTAP, 50 μ L of 20 mM Cholesterol and 50 μ L of 10 mM DSPE–PEG-2000 or DSPE–PEG-AA were combined. After evaporating the chloroform, the residual lipids were dispersed in 1.0 mL of d-H₂O. The particle size of LPC NPs was determined using a Malvern ZetaSizer Nano series (Westborough, MA). TEM images of LPC NPs were acquired using a JEOL 100CX II TEM (JEOL, Japan). The LPC NPs were negatively stained with 2% uranyl acetate.

Biodistribution. The mice were administered a single dose of 1.0 mg/kg Pt CDDP and LPC NPs. Each group contained five mice, which were sacrificed 4 h following injection. Tissue samples were digested by concentrated nitric acid overnight at room temperature and processed according to the procedure reported previously in the literature.^{27,28} The concentration of Pt was measured using ICP-MS.

In Vivo Anticancer Efficacy. Animals were maintained in the Center for Experimental Animals (an AAALAC accredited experimental animal facility) at the University of North Carolina. All procedures involving experimental animals were performed in accordance with the protocols approved by the University of North Carolina Institutional Animal Care and Use committee and conformed to the Guide for the Care and Use of Laboratory Animals (NIH publication No. 86-23, revised 1985). Female athymic nude mice, 5–6 weeks old and weighing 18–22 g were supplied by the University of North Carolina animal facility. A total of 5×10^6 A375M cells were injected subcutaneously into the mice. After 10 days, the mice were randomly divided into four groups (4–6 mice per group). The mice were treated with weekly iv injections of CDDP and LPC NPs and saline as a control. A dose of 1.0 mg/kg Pt was administered. Thereafter, tumor growth and body weight were monitored. Tumor volume was calculated using the following formula: $TV = (L \times W^2)/2$, with W being smaller than L . Finally, mice were sacrificed using a CO₂ inhalation method. After the therapeutic experiment was done, blood samples were collected and allowed to clot for 2 h at room temperature. Serum was obtained through centrifugation for 20 min at 2000g. For liver and renal function experiments, the levels of aspartate aminotransferase, alanine aminotransferase, and blood urea nitrogen in the serum were measured. Major organs were collected after treatment and were formalin fixed and processed for routine H&E staining using standard methods. Images were collected using a Nikon light microscope (Nikon).

After the A375M tumor reached 600 mm³, the mice were treated with two weekly iv injections of LPC NPs at a dose of 3.0 mg/kg Pt. Seven days post the last injection, the mice were sacrificed and the tumors were assayed with TUNEL.

TUNEL Assay. The tumors were fixed in 4.0% paraformaldehyde (PFA), paraffin-embedded, and sectioned at the UNC Lineberger Comprehensive Cancer Center Animal Histopathology Facility. To detect apoptotic cells in tumor tissues, a TUNEL assay, using a DeadEnd Fluorometric TUNEL System (Promega, Madison, WI), was performed following the manufacturer's protocols. Cell nuclei that were fluorescently stained with green were defined as TUNEL-positive nuclei. TUNEL-positive nuclei were monitored using a fluorescence microscope (Nikon, Tokyo, Japan). The cell nuclei were stained with 4, 6-diamidino-2-phenyl-indole (DAPI) Vectashield (Vector Laboratories, Inc., Burlingame, CA). TUNEL-positive cells in three slides and captured in images taken at 40 \times magnification were counted to quantify apoptosis.

In Vivo Neighboring Effect Study. To study the neighboring effect, the LPC NPs were labeled with Dil dye (Sigma-Aldrich, St. Louis, MO) and administered to nude mice bearing A375M tumors at a single dose of 1.0 mg/kg Pt. Each group contained three mice that were sacrificed 24 h post injection. The organs and tumor sections were prepared by the procedure described in the TUNEL assay in Supporting Information. The distribution of NPs (red) and TUNEL positive cells (green) were observed using a fluorescence microscope (Nikon, Tokyo, Japan). The distance between two cells was measured using the NIS-Elements Microscope Imaging Software (Nikon Corp., Tokyo, Japan).

To observe the distribution of LPC NPs in liver, the sections were incubated with a 1:250 dilution of CD68 primary antibody (Abcam, Cambridge, MA) at 4 °C overnight followed by incubation with FITC-labeled secondary antibody (1:200, Santa Cruz, CA) for 1 h at room temperature. The sections were also stained by DAPI and covered with a coverslip. The sections were observed using a Nikon light microscope (Nikon Corp., Tokyo, Japan).

The CDDP–DNA adducts were detected using anti-CDDP modified DNA antibodies [CP9/19] (Abcam, Cambridge, MA). The sections were incubated with a 1:250 dilution of anti-CDDP modified DNA antibody [CP9/19] at 4 °C overnight followed by incubation with FITC-labeled goat anti-rat Ig antibody (1:200, Santa Cruz, CA) for 1 h at room temperature. The sections were also stained by DAPI and covered with a coverslip. The sections were observed using a Nikon light microscope (Nikon Corp., Tokyo, Japan).

In Vitro Neighboring Effect Study. A375M-GFP cells (2×10^5) were seeded in 6-well plates (Corning Inc., Corning, NY) 20 h before the beginning of the experiments. The cells were first treated with CDDP and LPC NPs (50 μ M Pt) at 37 °C for 4 h and then trypsinized. The A375M-GFP cells were mixed with A375M cells at the ratio of 1:10 (total cell number: 2×10^5) and reseeded into 6-well plates. After culturing for 48 h, the cells were stained with Hoechst 33342 (Sigma, St. Louis, MO) and Annexin V Alexa Fluor 568 Conjugate (Invitrogen, Carlsbad, CA). Cells stained with Alexa Fluor 568 Conjugate were observed with a fluorescence microscope (Nikon, Tokyo, Japan) and quantified using flow cytometry (Becton-Dickinson, Heidelberg, Germany). Results were processed using the Cellquest software (Becton-Dickinson).

Conflict of Interest: The authors declare no competing financial interest.

Supporting Information Available: Cell toxicity assay, cellular uptake, *in vitro* drug release in 50% FBS and cellular release of Pt drug and its cell toxicity. This material is available free of charge via the Internet at <http://pubs.acs.org>.

Acknowledgment. This work was supported by NIH grants CA129835, CA129421, CA151652, CA151455 and CA149363. We thank Kelly Racette for her assistance in manuscript preparation and Chin-Ying Chung and Gavin Robertson for providing A375M and A375M-GFP cell line.

REFERENCES AND NOTES

- Rosenber, B.; Vancamp, L.; Krigas, T. Inhibition of Cell Division in *Escherichia Coli* by Electrolysis Products from a Platinum Electrode. *Nature* **1965**, *205*, 698–699.
- Lebwohl, D.; Canetta, R. Clinical Development of Platinum Complexes in Cancer Therapy: An Historical Perspective and an Update. *Eur. J. Cancer* **1998**, *34*, 1522–1534.
- Drayton, R. M.; Catto, J. W. F. Molecular Mechanisms of Cisplatin Resistance in Bladder Cancer. *Expert Rev. Anticancer Ther.* **2012**, *12*, 271–281.
- Liang, X. J.; Meng, H.; Wang, Y.; He, H.; Meng, J.; Lu, J.; Wang, P. C.; Zhao, Y.; Gao, X.; Sun, B.; et al. Metallofullerene Nanoparticles Circumvent Tumor Resistance to Cisplatin by Reactivating Endocytosis. *Proc. Natl. Acad. Sci. U.S.A.* **2010**, *107*, 7449–7454.
- Go, R. S.; Adjei, A. A. Review of the Comparative Pharmacology and Clinical Activity of Cisplatin and Carboplatin. *J. Clin. Oncol.* **1999**, *17*, 409–422.
- Farokhzad, O. C.; Langer, R. Nanomedicine: Developing Smarter Therapeutic and Diagnostic Modalities. *Adv. Drug Delivery Rev.* **2006**, *58*, 1456–1459.
- Davis, M. E.; Chen, Z.; Shin, D. M. Nanoparticle Therapeutics: An Emerging Treatment Modality for Cancer. *Nat. Rev. Drug Discovery* **2008**, *7*, 771–782.
- Klibanov, A. L.; Maruyama, K.; Torchilin, V. P.; Huang, L. Amphiphatic Polyethyleneglycols Effectively Prolong the Circulation Time of Liposomes. *FEBS Lett.* **1990**, *268*, 235–237.
- Farokhzad, O. C.; Karp, J. M.; Langer, R. Nanoparticle–Aptamer Bioconjugates for Cancer Targeting. *Expert Opin. Drug Delivery* **2006**, *3*, 311–324.

10. Banerjee, R.; Tyagi, P.; Li, S.; Huang, L. Anisamide-Targeted Stealth Liposomes: A Potent Carrier for Targeting Doxorubicin to Human Prostate Cancer Cells. *Int. J. Cancer* **2004**, *112*, 693–700.
11. Li, Z.; Huang, P.; Zhang, X.; Lin, J.; Yang, S.; Liu, B.; Gao, F.; Xi, P.; Ren, Q.; Cui, D. Rgd-Conjugated Dendrimer-Modified Gold Nanorods for *In Vivo* Tumor Targeting and Photothermal Therapy. *Mol. Pharmaceutics* **2009**, *7*, 94–104.
12. Zhang, C. F.; Jugold, M.; Woenne, E. C.; Lammers, T.; Morgenstern, B.; Mueller, M. M.; Zentgraf, H.; Bock, M.; Eisenhut, M.; Semmler, W.; *et al.* Specific Targeting of Tumor Angiogenesis by Rgd-Conjugated Ultrasmall Superparamagnetic Iron Oxide Particles Using a Clinical 1.5-T Magnetic Resonance Scanner. *Cancer Res.* **2007**, *67*, 1555–1562.
13. Maeda, H.; Wu, J.; Sawa, T.; Matsumura, Y.; Hori, K. Tumor Vascular Permeability and the Epr Effect in Macromolecular Therapeutics: A Review. *J. Controlled Release* **2000**, *65*, 271–284.
14. Cabral, H.; Matsumoto, Y.; Mizuno, K.; Chen, Q.; Murakami, M.; Kimura, M.; Terada, Y.; Kano, M. R.; Miyazono, K.; Uesaka, M.; *et al.* Accumulation of Sub-100 Nm Polymeric Micelles in Poorly Permeable Tumours Depends on Size. *Nat. Nano* **2011**, *6*, 815–823.
15. Chauhan, V. P.; Stylianopoulos, T.; Martin, J. D.; Popović, Z.; Chen, O.; Kamoun, W. S.; Bawendi, M. G.; Fukumura, D.; Jain, R. K. Normalization of Tumour Blood Vessels Improves the Delivery of Nanomedicines in a Size-Dependent Manner. *Nat. Nanotechnol.* **2012**, *7*, 383–388.
16. Burger, K. N.; Staffhorst, R. W.; de Vijlder, H. C.; Velinova, M. J.; Bomans, P. H.; Frederik, P. M.; de Kruijff, B. Nanocapsules: Lipid-Coated Aggregates of Cisplatin with High Cytotoxicity. *Nat. Med.* **2002**, *8*, 81–84.
17. Hamelers, I. H.; de Kroon, A. I. Nanocapsules: A Novel Lipid Formulation Platform for Platinum-Based Anti-Cancer Drugs. *J. Liposome Res.* **2007**, *17*, 183–189.
18. Khiati, S.; Luvino, D.; Oumzil, K.; Chauffert, B.; Camplo, M.; Barthelemy, P. Nucleoside-Lipid-Based Nanoparticles for Cisplatin Delivery. *ACS Nano* **2011**, *5*, 8649–8655.
19. Kieler-Ferguson, H. M.; Fréchet, J. M. J.; Szoka, F. C., Jr Clinical Developments of Chemotherapeutic Nanomedicines: Polymers and Liposomes for Delivery of Camptothecins and Platinum (II) Drugs. *Wiley Interdiscip. Rev. Nanomed. Nanobiotechnol.* **2013**, *5*, 130–138.
20. Dhar, S.; Gu, F. X.; Langer, R.; Farokhzad, O. C.; Lippard, S. J. Targeted Delivery of Cisplatin to Prostate Cancer Cells by Aptamer Functionalized Pt(IV) Prodrug-PLGA-Peg Nanoparticles. *Proc. Natl. Acad. Sci. U.S.A.* **2008**, *105*, 17356–17361.
21. Li, X.; Wang, L.-K.; Wang, L.-W.; Han, X.-Q.; Yang, F.; Gong, Z.-J. Cisplatin Protects against Acute Liver Failure by Inhibiting Nuclear Hmgb1 Release. *Int. J. Mol. Sci.* **2013**, *14*, 11224–11237.
22. Basu, A.; Krishnamurthy, S. Cellular Responses to Cisplatin-Induced DNA Damage. *J. Nucleic Acids* **2010**, *2010*.
23. Kang, T.-H.; Lindsey-Boltz, L. A.; Reardon, J. T.; Sancar, A. Circadian Control of Xpa and Excision Repair of Cisplatin-DNA Damage by Cryptochrome and Herc2 Ubiquitin Ligase. *Proc. Natl. Acad. Sci. U.S.A.* **2010**, *107*, 4890–4895.
24. Newman, M. S.; Colbern, G. T.; Working, P. K.; Engbers, C.; Amantea, M. A. Comparative Pharmacokinetics, Tissue Distribution, and Therapeutic Effectiveness of Cisplatin Encapsulated in Long-Circulating, Pegylated Liposomes (Spi-077) in Tumor-Bearing Mice. *Cancer Chemother. Pharmacol.* **1999**, *43*, 1–7.
25. Comenge, J.; Sotelo, C.; Romero, F.; Gallego, O.; Barnadas, A.; Parada, T. G.-C.; Domínguez, F.; Puntes, V. F. Detoxifying Antitumoral Drugs via Nanoconjugation: The Case of Gold Nanoparticles and Cisplatin. *PLoS One* **2012**, *7*, e47562.
26. Guo, S.; Miao, L.; Wang, Y.; Huang, L. Unmodified Drug Used as a Material to Construct Nanoparticles: Delivery of Cisplatin for Enhanced Anti-Cancer Therapy. *J. Controlled Release* **2013**, submitted for publication.
27. Graf, N.; Bielenberg, D. R.; Kolishetti, N.; Muus, C.; Banyard, J.; Farokhzad, O. C.; Lippard, S. J. Alpha(V)Beta(3) Integrin-Targeted PLGA-Peg Nanoparticles for Enhanced Anti-Tumor Efficacy of a Pt(IV) Prodrug. *ACS Nano* **2012**, *6*, 4530–4539.
28. McGahan, M. C.; Tyczkowska, K. The Determination of Platinum in Biological Materials by Electrothermal Atomic-Absorption Spectroscopy. *Spectrochim. Acta, Part B* **1987**, *42*, 665–668.